Counteranion Dependent Protonation and Aggregation of Tetrakis(4-sulfonatophenyl)porphyrin in Organic Solvents

Giovanna De Luca, Andrea Romeo, and Luigi Monsù Scolaro*

Dipartimento di Chimica Inorganica, Chimica Analitica e Chimica Fisica, Università di Messina, Salita Sperone 31, 98166 Vill. S. Agata, Messina, Italy

Received: June 7, 2005; In Final Form: October 3, 2005

The tetrabutylammonium salt of 5,10,15,20-tetrakis(4-sulfonatophenyl)porphyrin (TPPS) is soluble in dichloromethane, and the general properties of this compound have been investigated as function of various added acids HX (X = Cl, Br, I, CF_3COO, CF_3SO_3, TFPB) through UV−vis absorption spectroscopy, steady state fluorescence emission, and resonance light-scattering (RLS) techniques. Upon addition of HX, the initial monomeric free base TPPS is readily converted in an aggregated species, whose spectroscopic features are independent of the nature of the counteranion X. All the spectroscopic evidence suggest a J-type arrangement of chromophores in this aggregate, involving strong hydrogen bonds, electrostatic, and dispersive interactions. In the specific case of chloride and bromide, in the presence of a TBAX excess, the addition of the corresponding acid leads to a monomeric ion-pair between the TBA cations and the diacid TPPS, whose central core is strongly interacting with the halide. On further increasing the acid concentration in these latter solutions, fully protonated species are formed that eventually start to aggregate.

Introduction

Aggregation is a general phenomenon that has a deep impact on many physicochemical properties of porphyrins.[1] Aggregated species play a key role in many different systems, e.g., in light-harvesting antennas of photosynthetic plants and bacteria,[2,3] and their optical features can be potentially exploited, e.g., for their nonlinear optical properties.[4,5] Therefore, the possibility of controlling the size, the structural, and spectroscopic features of these arrays of chromophores is an important research goal.

In the past decade, the water-soluble 5,10,15,20-tetrakis(4-sulfonatophenyl)porphyrin (TPPS) has received much attention because its diprotonated form aggregates, yielding well-defined nanorods of J-aggregated porphyrins[6] possessing favorable photophysical properties that make them potentially applicable in optoelectronics.[7,8] The free base TPPS is tetra-anionic because of the presence of four negatively charged sulfonate residues on the mesophenyl substituents groups. At neutral pH values, this molecule exists as a monomeric free base ($pK_a \sim 4.9$)[9] due to electrostatic repulsion. By lowering the pH below 4, the zwitterionic diacid species is prevalently formed. On increasing the acidity and the ionic strength of the solutions, aggregation largely occurs and both H- and J-aggregates have been reported so far.[10−29] The exciton theory developed by Kasha has been generally adopted for interpreting the experimental splitting of the absorption bands in such systems.[30−32] Two limiting geometrical arrangements, H- (*face-to-face*) or J-type (*side-by-side*), can be considered, leading to a higher energy (hypsochromic shift) and a lower energy transition (bathochromic shift), respectively, in comparison with the initial monomer. So far, the general accepted model for the J-aggregate is based on a network of electrostatic and hydrogen bonding interactions, which involve the negatively charged sulfonate groups and the positively charged inner nitrogen core. A peculiar spectroscopic feature for these aggregates is a narrow and largely red-shifted B band (the J band), which has been interpreted in terms of exciton delocalization over a large number of monomer units.[33] Apart from investigations in simple acidic media, the occurrence of both J- and H-aggregates has been reported in many complex or confined environments.[34−45]

Recently, we have focused our interest on aggregation of tetra-aryl-substituted porphyrins in organic solvents because, despite many reports on aggregation phenomena in aqueous or mixed aqueous−organic phase, very few investigations have been devoted to nonaqueous environments. Previous studies[46,47] have pointed out an expected dependence of the protonation and aggregation behavior on the nature of the porphyrins but, quite unexpectedly, also on the nature of the acid needed to foster aggregation. In particular, in agreement with recent theoretical calculations,[48] both protonation and subsequent aggregation exhibit spectroscopic features that markedly depend on the nature of the counteranion.

Here we report on the protonation and aggregation properties of the tetrabutylammonium salt of TPPS[49] in dichloromethane. We anticipate that, even in this case, a complex pattern of behavior can be observed and the main spectroscopic features are affected only by the presence of specific counteranions.

Experimental Section

Chemicals. All the tetrabutylammonium (TBA) salts, the hydrogen halides, trifluoroacetic acid, and trifluoromethanesulfonic acid were of the highest commercial grade available (Aldrich) and were used as received without further purification. Sodium tetrakis[3,5-bis(trifluoromethyl)phenyl]borate (NaTFPB) and the corresponding acid (HTFPB) were prepared according to a literature procedure.[50] (TBA)TFPB salt was prepared from NaTFPB by cation exchange on a Dowex 50 W resin.

5,10,15,20-Tetrakis(4-sulfonatophenyl)porphyrin tetrasodium salt (Na_4TPPS) was purchased from Aldrich Chemical Co. and

* Corresponding author. E-mail: monsu@chem.unime.it. Telephone: +39 090 676 5711. Fax: +39 090 393756.

10.1021/jp0530348 CCC: $33.50
Published on Web 03/23/2006

used as received. The TBA salt was prepared from Na_4TPPS by adding the stoichiometric amount of TBACl to a porphyrin aqueous solution. Water was removed with a rotary evaporator, and the solid was redissolved in dichloromethane. This dark-red solution was filtered over cellulose powder to remove NaCl precipitate. The solid porphyrin was recovered after removing the solvent. Anal. Calcd for $C_{108}H_{170}N_8O_{12}S_4$: C, 68.24; H, 9.01; N, 5.89. Found: C, 67.85; H, 9.32; N, 5.57.

The stock solutions, obtained by dissolving the porphyrin in dichloromethane (Sigma, spectrophotometric grade), were stored in the dark and used within a week from preparation. The range of concentration ($5-10 \times 10^{-6}$ M) used in our experiments was determined spectrophotometrically by using the molar extinction coefficient at the Soret maximum ($(TBA)_4TPPS/CH_2Cl_2$: 6.03×10^5 M^{-1} cm^{-1}, $\lambda = 420$ nm).

In the case of hydrogen halides, acid vapors were injected to a prefixed volume of porphyrin solution of known concentration (2−2.5 mL, [porphyrin] = 2−6 μM). A homemade glass kit connected directly to a reservoir of concentrated acid solution was used. The protonation process and the conversion of the porphyrin into the various aggregated species were directly monitored through UV−vis spectroscopy in 1-cm absorption cells. The total amount of added acid was roughly estimated from independent back-titration of dichloromethane solutions of hydrogen halides, using aqueous NaOH. All the other acids were added by injecting small amount of neat acid or diluted dichloromethane solutions from a microliter syringe. In all the cases, the concentration of the acid stock solutions was high enough to prevent dilution effect. All the experiments were repeated at least three times to check for reproducibility. In the case of aggregated species, precipitation was detected upon prolonged standing.

Spectroscopic Methods. UV−Vis absorption spectra were measured on a Hewlett-Packard model HP 8453 diode array spectrophotometer. An UV filter (Hoya glass type UV-34; cutoff: 340 nm) was used in all measurements in order to cut off the UV component of the spectrophotometer lamp, avoiding the formation of HCl by photodecomposition of dichloromethane. Fluorescence (emission and excitation spectra) and resonance light-scattering (RLS) experiments were performed on a Jasco model FP-750 spectrofluorimeter equipped with a Hamamatsu R928 photomultiplier. For RLS experiments, a synchronous scan protocol with a right-angle geometry was adopted.[51] Fluorescence and RLS spectra were not corrected for absorption of the samples.

Results

The tetrabutylammonium salt of the title porphyrin $(TBA)_4TPPS$ is readily soluble in organic solvents such as dichloromethane or chloroform, displaying a very sharp and intense B band accompanied by four weaker Q bands in the absorption spectra. Solutions are strongly fluorescent, showing the two-band emission typical for this kind of fluorophore, and the RLS profile is almost superimposable onto that of the neat solvent. All these features point to the monomeric nature of porphyrins in these conditions.

Interaction of $(TBA)_4TPPS$ with a Series of HX. When small amounts of the various acids HX (X = Cl, Br, I, CF_3COO, CF_3SO_3, TFPB) are added to the porphyrin solutions, a common pattern of behavior is observed. The UV−vis spectra show the gradual conversion of the monomer to a new species characterized by a broad, hypochromic, and red-shifted Soret band.[52] Figure 1 reports the observed spectral changes in the case of HCl. The fluorescence emission is almost totally quenched, and an intense feature is observed in the RLS spectra at the red edge portion of the absorption band (Figure 2). All this experimental evidence indicates the formation of aggregates in which the porphine core is diprotonated (H_2TPPS_{agg}).[53]

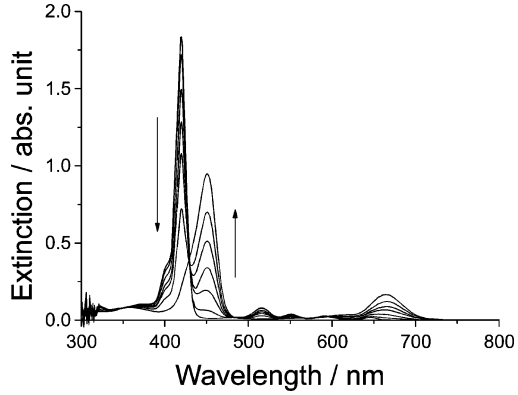

Figure 1. UV−Vis spectral changes following the stepwise addition of HCl to a dichloromethane solution of $(TBA)_4TPPS$ ([porphyrin] = 3 μM). The arrows mark the increase of acid concentration (up to [HCl] = 200 μM).

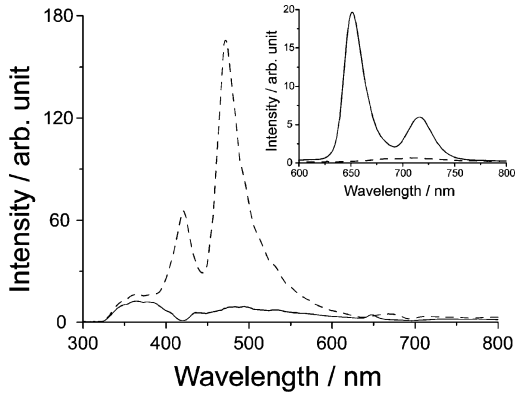

Figure 2. RLS spectra and fluorescence emission spectra (inset) for final species obtained by addition of HCl to a dichloromethane solution of $(TBA)_4TPPS$ (experimental conditions as in Figure 1): starting solution (solid line), H_2TPPS_{agg} (dashed line).

Effect of TBA Salts. The presence of an excess of TBACl (0.05 M) in the $(TBA)_4TPPS$ starting solution strongly affects the above-described behavior. In this case, the titration data point out the formation of a monomeric diacid form ($H_2TPPSCl_2$). The conversion of the free base porphyrin into a monomeric diacid form is supported by several findings: (i) the UV−vis spectra display the gradual formation of a new species (passing through a series of isosbestic points), characterized by a sharp and intense red-shifted Soret band accompanied by three Q bands, (ii) fluorescence emission, though deeply influenced, remains still intense, (iii) the presence of weak RLS profiles with wells due to photon loss at the wavelength corresponding to the absorption band (see Supporting Information).

These findings prompted us to investigate the possible disaggregating effect of TBA salts by "back-titrating" the preformed aggregates obtained by acidification of the free base solution with the corresponding TBAX.

When an excess of the TBACl salt is added to the corresponding aggregate, the broad Soret band sharpens (Figure 3), the fluorescence emission increases, and the RLS intensity decreases nearly to the signal observed for monomeric species, pointing to aggregates disruption (Figure 4). In the case of TBABr, the fluorescence emission is still considerably quenched and a moderately intense peak is evident in the RLS profiles. Even if more bromide salt is added with respect to the chloride

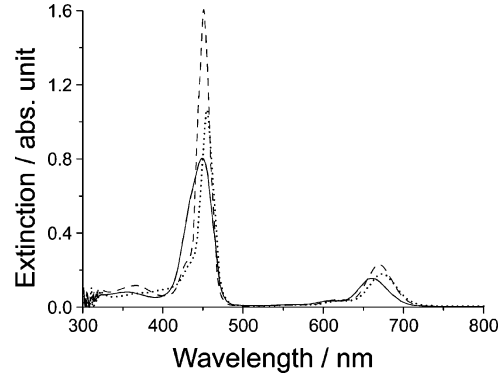

Figure 3. UV−Vis spectral changes upon TBAX additions (0.05 M) to the corresponding preformed porphyrin aggregate ([porphyrin] = 3 μM, [HCl] = 200 μM or [HBr] = 350 μM): H_2TPPS_{agg} (solid line), $H_2TPPSCl_2$ (dashed line), $H_2TPPSBr_2$ (dotted line).

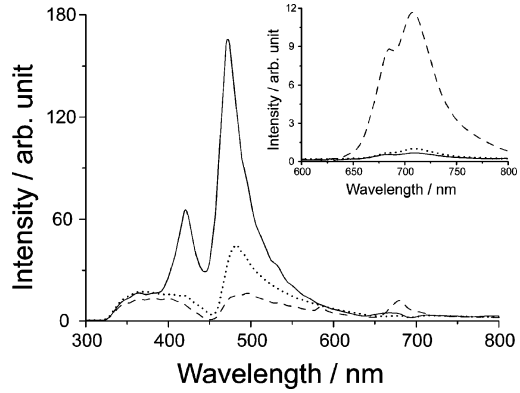

Figure 4. RLS and fluorescence emission (inset) spectra registered after TBAX additions (0.05 M) to the corresponding preformed porphyrin aggregate ([porphyrin] = 3 μM, [HCl] = 200 μM or [HBr] = 350 μM): H_2TPPS_{agg} (solid line), $H_2TPPSCl_2$ (dashed line), $H_2TPPSBr_2$ (dotted line).

system, the final solution still shows, together with $H_2TPPSBr_2$ monomeric species, the presence of small residual aggregates, which can explain the observed low fluorescence emission.

The data reported in Table 1 summarize the dependence of the spectroscopic features of the various species on the nature of the counteranion. The position and intensity of the Soret band and the corresponding fluorescence emissions are different for the two systems, according to the data already reported in the literature for TPP diacids[48] and for the acid-induced aggregates of TpyP isomers.[47]

Upon addition of different TBAX salts (X = I, CF_3SO_3, TFPB) to the corresponding preformed porphyrin aggregates, the Soret bands retain their positions even if exhibiting a certain extent of hypochromicity, while the fluorescence emissions are furthermore quenched and the RLS signals increase. All these findings suggest an increase of the aggregation extent in these systems.

Effect of Acid Excess. When more acid is added to the solutions of the monomeric diacid porphyrin derivatives, obtained in the presence of an excess of TBAX (X = Cl, Br), other phenomena can be observed. Figure 5 shows the UV−vis spectral changes that occur upon HCl addition to a $H_2TPPSCl_2$ solution. Initially, a new sharp but unsymmetrical band appears in the extinction spectrum at 433 nm, while the Q bands slightly blue-shift with respect to those of the monomeric diacid forms (Figure 5a). Again, the fluorescence emission is quenched and a medium intensity peak appears in the RLS spectra (Figure 6, dashed lines), accounting for a modest aggregation of this new species ($H_6TPPSCl_2$).

On further increasing HCl concentration, the Soret band becomes broad, hypochromic, and red-shifted (Figure 5b, λ_{max} = 458 nm). The fluorescence emission is almost completely quenched, while the RLS spectra evidence a strong resonant peak at 488 nm (Figure 6, dotted lines).

Differently, further HBr additions to the $H_2TPPSBr_2$ system evidence a subsequent aggregation stage with a quite short intermediacy of a protonated species, as shown by the changes in the extinction spectra (Figure 7). The sharp Soret band decreases in intensity and broadens asymmetrically forming a blue-shifted shoulder at 436 nm. Afterward, this latter feature evolves, displaying hypochromicity and giving a large tail at longer wavelengths. Moreover, the weak fluorescence emission of the starting species is totally quenched and the RLS spectra evidence very intense signals at 482 nm (Figure 7, inset).

Discussion

The porphyrin TPPS is water soluble and its behavior in aqueous solutions, e.g., dimer formation in the presence of cation−crown ether complexes or aggregation phenomena driven by pH, cationic species, and ionic strength has been largely investigated.[10−29]

This tetra-anionic species can be easily solubilized in organic solvents (e.g., dichloromethane or chloroform) as tetrabutylammonium salt, exploiting the formation of ion-pairs between the lipophilic tetrabutylammonium cation and the sulfonate groups of the porphyrin. Indeed, all the spectroscopic evidence collected on $(TBA)_4TPPS$ in dichloromethane point to the monomeric nature of such species in this environment. The presence of four Q bands is in agreement with the D_{2h} symmetry of the central porphine ring, typical of a free base form.[13] Scheme 1 reports the ion-pairs and aggregated species formed under the conditions investigated during this study.

Interaction of $(TBA)_4TPPS$ with a Series of HX. Recent studies on porphyrin diacids have clearly shown a dependence of the spectroscopic features of these species on the nature of the counteranion.[47,48] Under our experimental conditions, the spectroscopic properties of the final species obtained by treating $(TBA)_4TPPS$ solutions with the different HX (X = Cl, Br, I, CF_3COO, CF_3SO_3, TFPB) do not show any counteranion dependence. The observed collapse of the Q bands number from four to three points to the initial porphyrin core protonation, which implies the change in symmetry of the molecule from D_{2h} (free base) to D_{2d} (diacids). The B band is broader (e.g., 1200 cm^{-1}, fwhm, for the chloride) with respect to the starting monomer (811 cm^{-1}, fwhm), suggesting, together with the large RLS peaks, the aggregated nature of these species.[54] Analogously with what has been reported in aqueous solutions, once the zwitterionic H_2TPPS diacid species has formed, stabilizing interactions can occur between the positively charged core of a porphyrin unit and the negative sulfonate groups of a neighboring one, leading to the formation of aggregated species (H_2TPPS_{agg}). It is worth noting that the initial zwitterionic diacid species H_2TPPS should bind counteranions quite strongly, through hydrogen bonds with the central N−H pyrrole groups (see below). This process is expected to be largely enhanced in low-polarity solvents with respect to water. The structural disposition of the porphyrins in the aggregate can be ascribed to a J-type geometry, analogous with the behavior exhibited in aqueous solution and as suggested by the strong enhancement of RLS signals.[24,47,55,56] In the present case, the sulfonate groups efficiently compete with any other anion for the porphyrin core, achieving also more effective stacking interactions between adjacent porphyrins (route a in Scheme 1). Therefore, in line

TABLE 1: UV−Vis Absorption, Emission, and RLS Features of TPPS(TBA)$_4$ Porphyrin and Derived Species in the Presence of Various HX in Dichloromethane at 298 K

X	species	B bands (λ/nm)	Q bands (λ/nm)				emission maxima (λ/nm)		RLS
	$(TBA)_4TPPS$	420	516	551	591	646	651	717	
Cl^-	H_2TPPS_{agg} [a]	451		559	612	661	684	711	473
	H_2TPPSX_2 [b]	451		565	617	670	685	708	
	H_6TPPSX_2	433		570	619	664	684	709	464 (weak)
	H_6TPPSX_{2agg}	458			625	682	684	712	488
Br^-	H_2TPPS_{agg} [a]	451		560	612	666	684	711	472
	H_2TPPSX_2 [b]	455		567	618	673	684	709	
	H_6TPPSX_{2agg}	436,[c] 454			615	668			482
I^-	H_2TPPS_{agg} [a]	451			611	663	685	711	474
CF_3COO^-	H_2TPPS_{agg} [a]	451		558	612	667	685	712	475
	H_6TPPSX_{2agg}	443			598	654	−	−	473
$CF_3SO_3^-$	H_2TPPS_{agg} [a]	451		558	615	666	685	712	475
$TFPB^-$	H_2TPPS_{agg} [a]	451		558	612	667	685	712	475

[a] $\{2(TBA^+)\cdot(H_2TPPS^{2-})\}_{agg}$. [b] $\{4(TBA^+)\cdot(H_2TPPSX_2^{4-})\}$. [c] Shoulder.

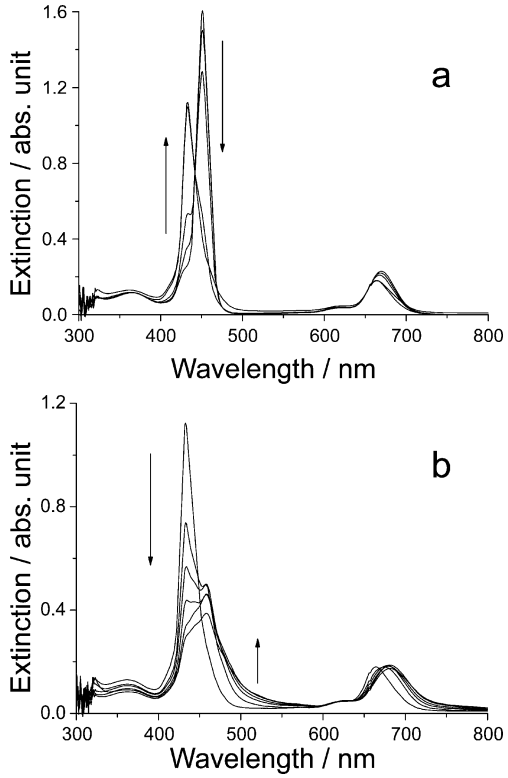

Figure 5. UV−Vis spectral changes following the further stepwise addition of HCl to a dichloromethane solution of $H_2TPPSCl_2$. The arrows mark the increase of acid concentration: (a) from [HCl] = 200 μM to 1 mM, and (b) from [HCl] = 1 mM to 2.5 mM). ([porphyrin] = 3 μM, [TBACl] = 0.05 M).

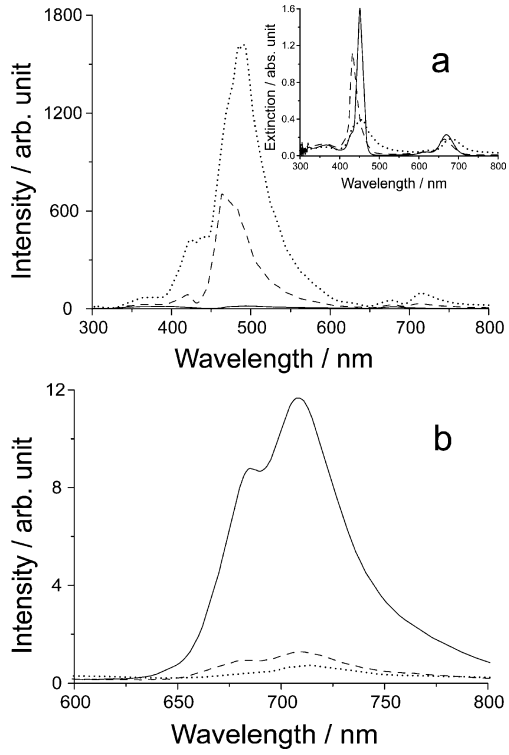

Figure 6. RLS (a), UV−Vis (a, inset) and fluorescence emission (b) spectra of the $H_2TPPSCl_2$ (solid line), $H_6TPPSCl_2$ (dashed line), and $H_6TPPSCl_{2agg}$ (dotted line) species. Experimental conditions as in Figure 5.

with the absence of detectable intermediate species in the corresponding spectral changes (see Figure 1), the monomeric diacid $\{4TBA^+\cdot H_2TPPSX_2^{4-}\}$ ion-pair is not stable under these experimental conditions and very rapidly evolves into the corresponding aggregate (Figure 8).

The model proposed for the aggregate structure does not involve any other species apart from the diprotonated porphyrin molecules (and the balancing TBA cations) and could, therefore, explain the experimentally observed lack of dependence of the spectral features on the nature of the counteranion. Interestingly, the UV−vis spectra of the J-aggregated TPPS in this organic solvent is rather different from that reported in aqueous solution, where a $\Delta\lambda = +55$ nm has been usually observed with respect to the corresponding diacid monomeric form.[11,13] In aqueous solutions, the Soret band of the diacid TPPS ($\lambda = 434$ nm) does not display any dependence on the counteranion[10,11,24,55] due to the low degree of hydrogen-bonding interactions between the protonated core and the anions. Consequently, in water, the measured and reported shift is between a real zwitterionic diacid monomer and the J-aggregate. In our case, it is rather difficult to determine the value of the shift with respect to the isolated monomeric H_2TPPS species in dichloromethane because this species is actually not stable and it is always strongly associated as an ion-pair with the counteranions, affecting the corresponding optical properties. Another striking difference is the broadening of the band with respect to the usually sharp J-absorption band for J-aggregated TPPS in water (244 cm^{-1}, fwhm).[20] All of these observed discrepancies seem to suggest

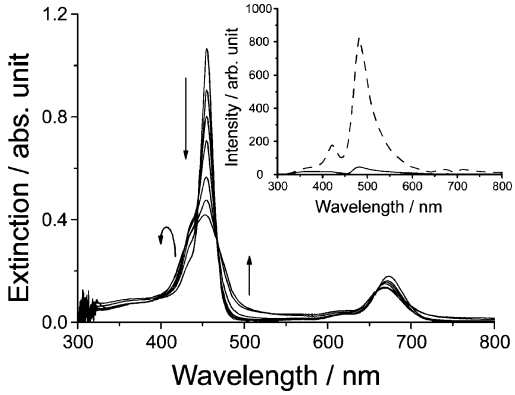

Figure 7. UV−Vis spectral changes following the stepwise addition of HBr to a dichloromethane solution of $H_2TPPSBr_2$, the arrows marking the increase of acid concentration (see text). Inset: RLS spectra of $H_2TPPSBr_2$ (solid line) and of the corresponding $H_6TPPSBr_{2agg}$ (dashed line). ([porphyrin] = 3 μM, [TBABr] = 0.05 M, [HBr] = 350−3000 μM).

SCHEME 1: Protonation and Aggregation General Behavior for the TPPS Porphyrin in the Presence of Various Acids and TBAX (X = Cl, Br) Salts in Dichloromethane

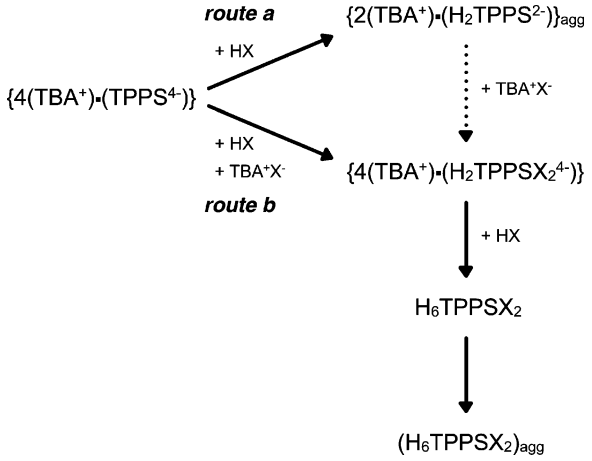

a role for the bulky TBA ions in the overall structural arrangement. Differently from our case, the assembling of different J-aggregates in aqueous solutions is surely mediated by small cations (sodium or potassium),[22,57] which closely bridge different arrays through the sulfonate groups not directly involved in the main porphyrin−porphyrin interaction. Anyway, the observation of a narrow J-band is rather rare, and usually large extinction features have been observed, which are often largely affected by resonant light-scattering components.[47,58,59]

Effect of TBA Salts. In the presence of TBACl excess, no aggregation has been detected upon HCl addition, and the spectroscopic features of the new species suggest the formation of a monomeric diacid derivative in which the protonated porphine core strongly interacts with two chloride anions ($H_2TPPSCl_2$). To determine if the TBA cation plays any role, different TBA salts have been added to the preformed aggregate obtained by acidification of $(TBA)_4TPPS$ with the corresponding acids. Our experimental data show that, only in the case of TBACl and TBABr, disaggregation is observed (route b, Scheme 1), with a smaller effectiveness for the bromide salt. On the contrary, aggregation is fostered by the other TBA salts. These findings allowed us to safely rule out the involvement of TBA cation and point to a role of the anions in this process.

Recently, DFT and TDDFT calculations on the diacid $\{(H_2TPP^{2+})(X^-)_2\}$ (X = F, Cl, Br, I) species have suggested

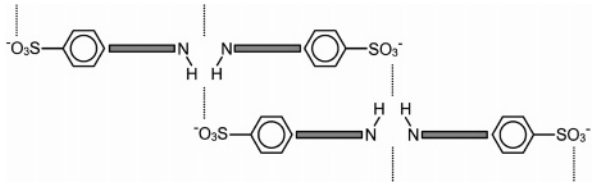

Figure 8. Pictorial sketch of a side view of the proposed model for the J-aggregation of H_2TPPS (i.e., H_2TPPS_{agg}) through the intermediacy of the peripheral sulfonate groups (charges on the central nitrogen atoms and saddling distortion have been omitted for clarity; N−H bonds belong to opposite pyrrole rings).

that covalent interactions make an important contribution to the total energy for the hydrogen bonding between the protonated pyrrole groups and the balancing counteranions.[48] The protonation of the TPP core causes remarkable distortion and phenyl group twisting. Furthermore, a splitting of the occupied Gouterman orbitals results from a strong interaction between the π systems of the central porphine and of the substituent groups. According to this study, the halide lone-pairs orbitals together with the Gouterman orbitals should be the highest occupied molecular orbitals, accounting for the observed dependence of the spectroscopic properties on the nature of the halide. These results also indicate for the chloride and bromide the highest ability to form tight-contact ion-pairs with respect to the other anions used in the present study. Hence, the formation of such ion-pairs between the halides and the TPPS protonated core can be hypothesized in the presence of an excess of TBACl and TBABr, leading to species ($H_2TPPSCl_2$ and $H_2TPPSBr_2$, respectively) whose diprotonated core is no longer available to interact with the negative sulfonate groups of adjacent molecules.[60] The bromide derivative exhibits a bathochromic shift $\Delta\lambda = +4$ nm with respect to the chloride derivative, analogous to what was reported ($\Delta\lambda = +5$ nm) for the corresponding diacid forms of TPP in the same solvent.[48]

Formation and Aggregation of Fully Protonated Species. On further adding HCl (or HBr) to the corresponding monomeric porphyrin diacids, other protonation steps beside that involving the porphyrin core become evident (route b in Scheme 1). Actually, assuming the sulfonate groups being unprotonated in the monomeric diacid species, it can be hypothesized that their protonation could take place at higher acid concentration. This leads to the formation of the fully protonated porphyrins (H_6TPPSX_2) whose porphine core strongly interacts with the counteranions, affecting their optical properties. This formally neutral species eventually aggregates. On the contrary, the formation of the fully protonated form of TPPS has already been reported in aqueous solution under strongly acidic conditions ([HCl] > 6 M), where it does not aggregate.[61]

Unlike the chloride case, it is not possible to distinguish between the protonation stage and the following aggregation process in the bromide system, probably due to a different influence of the two counteranions in stabilizing the fully protonated species in solution and/or in facilitating the subsequent aggregation step.

A hypothetical model for the J-type structure, which can be envisaged for these fully protonated aggregates, is reported in Figure 9. Actually, the different spectral features observed for the chloride and bromide systems can be explained by taking into account a role of the anions in the resulting network. In this case, hydrogen-bonding interactions between the peripheral sulfonic groups and the protonated central N−H residues are bridged by the halides.

The exciton theory predicts that the dipole−dipole interaction energy V for interacting chromophores changes according to

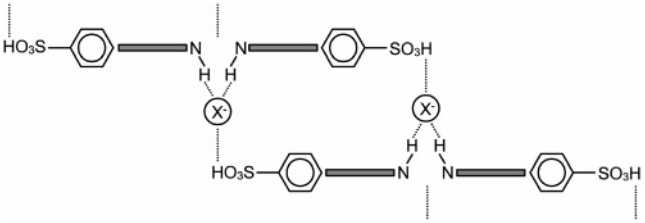

Figure 9. Pictorial sketch of a side view of the proposed model for the J-aggregation of the fully protonated H_6TPPSX_2 through the intermediacy of the peripheral sulfonic groups and halides (charges on the central nitrogen atoms and saddling distortion have been omitted for clarity; N−H bonds belong to opposite pyrrole rings).

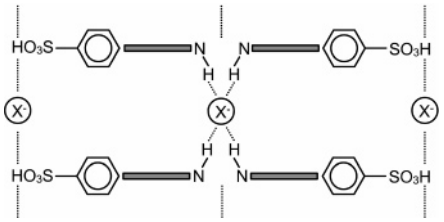

Figure 10. Pictorial sketch of a side view of the proposed model for the H-type aggregates of the fully protonated H_6TPPS in the presence of Br^- through the intermediacy of the peripheral sulfonic groups and halides (charges on the central nitrogen atoms and saddling distortion have been omitted for clarity; N−H bonds belong to opposite pyrrole rings).

geometrical factors,[30,31,33] and in particular, for a parallel arrangement of the transition moments, it can be expressed by the following equation:

$$V = -\frac{M^2}{r^3}(1 - 3\cos^2\theta)$$

in which M is the transition moment, r is the distance between the centers of the dipoles, and θ is the angle between the dipoles and the line connecting their centers. In the specific case of J-aggregates, the dipole moments are parallel and form an angle $\theta < \pi/2$.[62]

As already pointed out, the energy of both the B and Q bands are largely affected by the counteranions. Therefore, these latter species can exert a deep influence both on the values of the transition moment, as well as on the geometrical factors r and θ, leading to extensive modulation of the spectral properties of the final aggregates. This observation is in line with our recent results on the aggregation behavior of various acid species of isomeric tetra(pyridyl)porphyrins in dichloromethane[47] and with investigations on the counterions-dependent aggregation of tetrakis(4-carboxyphenyl)porphyrin (TCPP) in acid media.[55,56]

In the presence of the chloride anion, the J-type structure of the aggregates is supported by a 25 nm bathochromic shift of the Soret band for the aggregation of the $H_6TPPSCl_2$ species, while it is less evident for the bromide system, which displays only an asymmetrical broadening of the Soret band for the same process. Even if the same pattern of behavior can be analogously assumed for the two systems, it is not possible to exclude the formation of H-type aggregates in the presence of the bromide anion. Indeed, a possible structure for these kind of aggregates (Figure 10) could involve the presence of counteranions, accounting for the experimental evidence as well as the J-type model, as already proposed for the counterion dependent aggregation of tetrakis(4-carboxyphenyl)porphyrin.[55,56]

Concluding Remarks

As already pointed out, the protonation and aggregation properties of the title porphyrin in aqueous solutions have been widely investigated and documented. On the contrary, this is the first report on its behavior in organic solvents. Analogously to isomeric tetra(pyridyl)porphyrins, a quite complex pattern of behavior has been found in low-polarity solvents such as dichloromethane. Differently from aqueous solutions, counteranions play a major role in determining the final structure and the spectroscopic properties of the various protonated species. The observed aggregates exhibit a red-shifted band typical of J-type porphyrin arrangement and strong enhancement of the resonant light scattering. These aggregated species are stabilized by an interplay of hydrogen bonding, electrostatic, and dispersive forces, in which the counteranions can exert an important bridging role. The possibility of controlling the optical features of such species by varying the counteranion opens the way to exploit these aggregates as a model for photophysical processes in light-harvesting systems or for their potential application in material sciences and in nanotechnology.

Acknowledgment. We thank MIUR (COFIN 2004) for financial support.

Supporting Information Available: Figure SI1, SI2, and SI3 reporting the UV−vis titration and the fluorescence emission and RLS features relative to the interaction of HCl with $(TBA)_4TPPS$ in the presence of a TBACl excess. This material is available free of charge via the Internet at http://pubs.acs.org.

References and Notes

(1) White, W. I. In *The Porphyrins*; Dolphin, D., Ed.; Academic Press: New York, 1978; Vol. 5, p 303.

(2) Hu, X.; Schulten, K. *Phys. Today* **1997**, *50*, 28−34.

(3) Blankenship, R. E.; Olson, J. M.; Miller, M. Antenna Complexes from Green Photosynthetic Bacteria. In *Anoxygenic Photosynthetic Bacteria*; Blankenship, R. E., Madigan, M. T., Bauer, C. E., Eds.; Kluwer Academic Publishers: Dordrecht, 1995; pp 399−435.

(4) Spano, F. C.; Mukamel, S. *Phys. Rev. A* **1989**, *40*, 5783−5801.

(5) Suslick, K. S.; Rakow, N. A.; Kosal, M. E.; Chou, J.-H. *J. Porphyrins Phthalocyanines* **2000**, *4*, 407−413.

(6) Schwab, A. D.; Smith, D. E.; Rich, C. S.; Young, E. R.; Smith, W. F.; de Paula, J. C. *J. Phys. Chem. B* **2003**, *107*, 11339−11345.

(7) Schwab, A. D.; Smith, D. E.; Bond-Watts, B.; Johnston, D. E.; Hone, J.; Johnson, A. T.; de Paula, J. C.; Smith, W. F. *Nano Lett.* **2004**, *4*, 1261−1265.

(8) Collini, E.; Ferrante, C.; Bozio, R. *J. Phys. Chem. B* **2005**, *109*, 2−5.

(9) Kalyanasundaram, K. *Photochemistry of Polypyridine and Porphyrin Complexes*; Academic Press: London, 1992; p 482.

(10) Ohno, O.; Kaizu, Y.; Kobayashi, H. *J. Chem. Phys.* **1993**, *99*, 4128−4139.

(11) Ribo, J. M.; Crusats, J.; Farrera, J. A.; Valero, M. L. *J. Chem. Soc., Chem. Commun.* **1994**, 681−682.

(12) Akins, D. L.; Ozcelik, S.; Zhu, H. R.; Guo, C. *J. Phys. Chem.* **1996**, *100*, 14390−14396.

(13) Akins, D. L.; Zhu, H. R.; Guo, C. *J. Phys. Chem.* **1996**, *100*, 5420−5425.

(14) Collings, P. J.; Gibbs, E. J.; Starr, T. E.; Vafek, O.; Yee, C.; Pomerance, L. A.; Pasternack, R. F. *J. Phys. Chem. B* **1999**, *103*, 8474−8481.

(15) Gandini, S. C. M.; Gelamo, E. L.; Itri, R.; Tabak, M. *Biophys. J.* **2003**, *85*, 1259−1268.

(16) Kano, H.; Saito, T.; Kobayashi, T. *J. Phys. Chem. A* **2002**, *106*, 3445−3453.

(17) Kano, H.; Saito, T.; Kobayashi, T. *J. Phys. Chem. B* **2001**, *105*, 413−419.

(18) Kano, H.; Kobayashi, T. *J. Chem. Phys.* **2002**, *116*, 184−195.

(19) Kelbauskas, L.; Bagdonas, S.; Dietel, W.; Rotomskis, R. *J. Lumin.* **2003**, *101*, 253−262.

(20) Koti, A. S. R.; Taneja, J.; Periasamy, N. *Chem. Phys. Lett.* **2003**, *375*, 171−176.

(21) Lauceri, R.; Gurrieri, S.; Bellacchio, E.; Contino, A.; Scolaro, L. M.; Romeo, A.; Toscano, A.; Purrello, R. *Supramol. Chem.* **2000**, *12*, 193−202.

(22) Micali, N.; Mallamace, F.; Romeo, A.; Purrello, R.; Scolaro, L. M. *J. Phys. Chem. B* **2000**, *104*, 5897−5904.

(23) Micali, N.; Romeo, A.; Lauceri, R.; Purrello, R.; Mallamace, F.; Scolaro, L. M. *J. Phys. Chem. B* **2000**, *104*, 9416−9420.

(24) Pasternack, R. F.; Schaefer, K. F.; Hambright, P. *Inorg. Chem.* **1994**, *33*, 2062−2065.

(25) Maiti, N. C.; Ravikanth, M.; Mazumdar, S.; Periasamy, N. *J. Phys. Chem.* **1995**, *99*, 17192−17197.

(26) Ren, B.; Tian, Z. Q.; Guo, C.; Akins, D. L. *Chem. Phys. Lett.* **2000**, *328*, 17−22.

(27) Ribo, J. M.; Crusats, J.; Sagues, F.; Claret, J.; Rubires, R. *Science* **2001**, *292*, 2063−2066.

(28) Rotomskis, R.; Augulis, R.; Snitka, V.; Valiokas, R.; Liedberg, B. *J. Phys. Chem. B* **2004**, *108*, 2833−2838.

(29) Rubires, R.; Crusats, J.; El-Hachemi, Z.; Jaramillo, T.; Lopez, M.; Valls, E.; Farrera, J. A.; Ribo, J. M. *New J. Chem.* **1999**, *23*, 189−198.

(30) McRae, E. G.; Kasha, M. *J. Chem. Phys.* **1958**, *28*, 721−722.

(31) McRae, E. G.; Kasha, M. In *Physical Processes in Radiation Biology*; Augenstein, L., Mason, R., Rosenberg, B., Eds.; Academic Press: New York, 1964; pp 23−42.

(32) Ribo, J. M.; Bofill, J. M.; Crusats, J.; Rubires, R. *Chem.—Eur. J.* **2001**, *7*, 2733−2737.

(33) Knapp, E. W. *Chem. Phys.* **1984**, *85*, 73−82.

(34) Castriciano, M. A.; Romeo, A.; Villari, V.; Micali, N.; Scolaro, L. M. *J. Phys. Chem. B* **2004**, *108*, 9054−9059.

(35) Gandini, S. C. M.; Yushmanov, V. E.; Borissevitch, I. E.; Tabak, M. *Langmuir* **1999**, *15*, 6233−6243.

(36) Jiang, S. G.; Liu, M. H. *J. Phys. Chem. B* **2004**, *108*, 2880−2884.

(37) Koti, A. S. R.; Periasamy, N. *Chem. Mater.* **2003**, *15*, 369−371.

(38) Maiti, N. C.; Mazumdar, S.; Periasamy, N. *J. Porphyrin Phthalocyanines* **1998**, *2*, 369−376.

(39) Maiti, N. C.; Mazumdar, S.; Periasamy, N. *J. Phys. Chem. B* **1998**, *102*, 1528−1538.

(40) Paulo, P. M. R.; Costa, S. M. B. *Photochem. Photobiol. Sci.* **2003**, *2*, 597−604.

(41) Paulo, P. M. R.; Gronheid, R.; De Schryver, F. C.; Costa, S. M. B. *Macromolecules* **2003**, *36*, 9135−9144.

(42) Purrello, R.; Bellacchio, E.; Gurrieri, S.; Lauceri, R.; Raudino, A.; Scolaro, L. M.; Santoro, A. M. *J. Phys. Chem. B* **1998**, *102*, 8852−8857.

(43) Purrello, R.; Scolaro, L. M.; Bellacchio, E.; Gurrieri, S.; Romeo, A. *Inorg. Chem.* **1998**, *37*, 3647−3648.

(44) Xu, W.; Guo, H. Q.; Akins, D. L. *J. Phys. Chem. B* **2001**, *105*, 1543−1546.

(45) Zhang, L.; Yuan, J.; Liu, M. H. *J. Phys. Chem. B* **2003**, *107*, 12768−12773.

(46) Scolaro, L. M.; Romeo, A.; Castriciano, M. A.; De Luca, G.; Patanè, S.; Micali, N. *J. Am. Chem. Soc.* **2003**, *125*, 2040−2041.

(47) De Luca, G.; Romeo, A.; Scolaro, L. M. *J. Phys. Chem. B* **2005**, *109*, 7149−7158.

(48) Rosa, A.; Ricciardi, G.; Baerends, E. J.; Romeo, A.; Scolaro, L. M. *J. Phys. Chem. A* **2003**, *107*, 11468−11482.

(49) Hereafter, for the sake of simplicity, all the protonated and aggregated species will be reported omitting charges and TBA counterions, unless otherwise specified.

(50) Brookhart, M.; Grant, B.; Volpe, A. F. J. *Organometallics* **1992**, *11*, 3920−3922.

(51) Pasternack, R. F.; Collings, P. J. *Science* **1995**, *269*, 935−939.

(52) Extinction spectra also evidence the presence of three Q bands, in line with the protonation of the central nitrogen core and the change in the molecular symmetry from D_{2h} to D_{2d}.

(53) Upon increasing the concentration of HX, all the spectroscopic features (mainly RLS) suggest more aggregation to occur.

(54) Kano, K.; Takei, M.; Hashimoto, S. *J. Phys. Chem.* **1990**, *94*, 2181−2187.

(55) Choi, M. Y.; Pollard, J. A.; Webb, M. A.; McHale, J. L. *J. Am. Chem. Soc.* **2002**, *125*, 810−820.

(56) Doan, S. C.; Shanmugham, S.; Aston, D. E.; McHale, J. L. *J. Am. Chem. Soc.* **2005**, *127*, 5885−5892.

(57) Ribo, J. M.; Rubires, R.; El-Hachemi, Z.; Farrera, J. A.; Campos, L.; Pakhomov, G. L.; Vendrell, M. *Mater. Sci. Eng., C* **2000**, *11*, 107−115.

(58) Micali, N.; Mallamace, F.; Castriciano, M.; Romeo, A.; Scolaro, L. M. *Anal. Chem.* **2001**, *73*, 4958−4963.

(59) Scolaro, L. M.; Romeo, A.; Castriciano, M. A.; Micali, N. *Chem. Commun.* **2005**, 3018−3020.

(60) Acidification experiments carried out with various HX on $(TBA)_4$TPPS solutions containing an excess of TBACl show no dependence of the diacid's spectral features on the nature of the counteranions. This finding can be explained by considering that the chloride, which would form the strongest contact ion-pair, always competes successfully with other anions for the protonated core, affording invariably to the $\{4TBA^+ \cdot H_2\text{-}TPPSCl_2^{4-}\}$ species.

(61) Castriciano, M. A.; Romeo, A.; Villari, V.; Micali, N.; Scolaro, L. M. *J. Phys. Chem. B* **2003**, *107*, 8765−8771.

(62) Parkash, J.; Robblee, J. H.; Agnew, J.; Gibbs, E.; Collings, P.; Pasternack, R. F.; de Paula, J. C. *Biophys. J.* **1998**, *74*, 2089−2099.